Journal of Visualization, Vol. 5, No. 4 (2002) 381-388

Measurement of Aerodynamic Noise and Unsteady Flow Field around a Symmetrical Airfoil

Tomimatsu, S.*1 and Fujisawa, N.*2

*1 Graduate School of Niigata University, 8050 Ikarashi 2, Niigata 950-2181, Japan.
*2 Department of Mechanical and Production Engineering, Niigata University, 8050 Ikarashi 2, Niigata 950-2181, Japan.

Received 8 August 2001.
Revised 11 March 2002.

***Abstract*:** The purpose of this paper is to study the physics of aerodynamic noise generation from the symmetrical airfoil of NACA 0018 in a uniform flow. The relationship between the noise spectrum and the unsteady flow field around the airfoil is studied in an acoustic wind tunnel using flow visualization and PIV analysis. The discrete frequency noise was generated from the airfoil inclined at small angle of attack to the free stream. The flow visualization result indicates the presence of attached boundary layer over the suction side and the separated shear layer over the rear pressure side of the airfoil, when the discrete frequency noise is observed. It is found from the PIV analysis that a large magnitude of vorticity is generated periodically from the pressure side of the trailing edge and it develops into an asymmetrical vortex street in the wake of the airfoil. The periodicity of the shedding vortices was found to agree with that of the frequency of the generated noise.

***Keywords*:** aerodynamic noise, unsteady flow, visualization, PIV, airfoil.

1. Introduction

It is well known that the aerodynamic noise is generated from the airfoil by the interaction of the flow with the airfoil itself in a stream. The generation of such noise is often observed in turbo-machines, such as fan, blower, windmill and so on, so the study on the aerodynamic noise is very important in relation to the noise reduction in such turbo-machines. When the airfoil is located in a stream at relatively low Reynolds numbers, the laminar boundary-layer prevails over the airfoil surface and a discrete frequency noise is generated from the airfoil inclined at small angles of attack to the free-stream (Paterson et al., 1973). The basic mechanism of this noise generation was studied by Tam (1974), who suggested that the noise could be emitted from the self-exited feedback loop consisting of large-scale unstable disturbances in the boundary layer, the wake flow and the feedback acoustic waves. Later, further study was conducted to explore the physical aspects of the noise generation mechanism. Hayashi et al. (1995) measured the noise spectrum generated from the symmetrical airfoils and later the flow around the airfoils was visualized by dye injection technique in a water flow at the same Reynolds number (Hayashi et al., 1999). On the other hand, the velocity fluctuations over the airfoil were studied by Nakashima and Akishita (1995) using hot-wire anemometry. More recently, Fujisawa et al. (2001) conducted the surface flow visualization to clarify the flow condition over the airfoil under the noise generation using the shear-sensitive liquid crystal in comparison with the classical oil-film method. These experimental results indicate that the asymmetry of the flow condition over the airfoil surfaces is closely related to the discrete tone generation. However, the physics of the noise generation is still not clear, because the generation of such noise is closely related to the structure of the unsteady boundary layer over the airfoil, which has not been measured spatially due to the experimental difficulty using the point measurement techniques. It will be interesting in this aspect to study the flow structure

over the airfoil by particle imaging velocimetry (PIV), which will give us the instantaneous spatial information on the velocity field suitable for the study of such complex flow phenomenon.

The purpose of this paper is to study the physics of discrete tone generation from a symmetrical airfoil in a uniform flow. The noise spectrum analysis, flow visualization and PIV measurement are carried out in an acoustic wind tunnel and the relation between the aerodynamic noise and the instantaneous velocity field over the airfoil is studied based on the results.

2. Experimental Setup and Measuring Techniques

2.1 Measurement of Aerodynamic Noise

The experiments are carried out using an acoustic wind tunnel, which is described in Fig. 1. The velocity distributions of the wind tunnel are made uniform with an accuracy of ±1% by installing the honeycombs and screens, which results in the free-stream turbulence level of 1% at the test section. On the contrary, the noise level is kept small by installing the silencer and the sound absorbers on the wind tunnel. Therefore, the resultant noise level in the acoustic chamber (1 m apart from the main flow) is found to be as small as 50 dB at the free-stream velocity U_0 = 30 m/s. It is to be noted that the background noise level is 20 dB at the same experimental condition without the flow. For further details see Fujisawa et al. (2001).

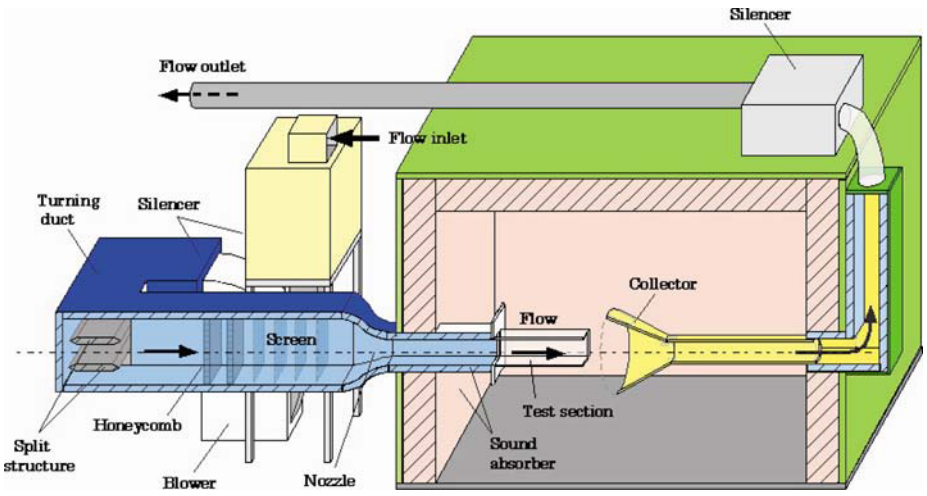

Fig. 1. Schematic illustration of acoustic wind tunnel.

The two-dimensional model of a symmetrical airfoil NACA 0018 is located at 200 mm from the inlet of the test section horizontally. The airfoil was made of aluminum and has a chord length of L = 80 mm. The airfoil can be rotated at the airfoil axis $x/L = 0$ to conduct the experiment at various angles of attack α to the free stream. The distance between the airfoil axis and the leading edge of the airfoil is 24 mm, which corresponds to $0.3L$.

The aerodynamic noise measurements are conducted in a closed test-section, which has a cross-sectional area of 190 × 190 mm with 500 mm long. The top and bottom walls are made of urethane material of 50 mm thickness to absorb the acoustic resonance, while the side walls are made of acrylic-resin. The spectrum of the aerodynamic noise was measured by using a sound level meter, which was inserted into the top wall to a position 10 mm from the inner-surface over the axis of the airfoil, so that the interference effect of the flow on the noise measurement effect is expected to be small. For details see Fujisawa et al. (2001). The output of the sound level meter was digitized by an AD converter to analyze the noise spectrum. All the experiments were conducted at free-stream velocity U_0 = 30 m/s, which corresponds to the Reynolds number Re ($= U_0 L/\nu$) = 1.6×10^5 (ν: viscosity of fluid).

2.2 Measurement of Velocity Field by PIV

The instantaneous velocity field around the airfoil at various angles of attack was measured by using the particle image velocimetry. Figure 2 shows the experimental apparatus for the flow visualization study and PIV analysis.

For flow visualization purposes, the smoke was generated by smoke machine and was injected at the inlet of the wind tunnel. The illumination was made by laser-light-sheet to visualize the two-dimensional velocity distributions in the vertical plane at the center of the test section. The lasers used in the present measurement are a pair of Nd:YAG lasers, which emit 532 nm wavelength light at a pulse repetition rate of 30 Hz. The highest pulse energy of these lasers is 50 mJ per pulse. The thickness of the light sheet is about 2 mm. The operation of the lasers is controlled by a pulse generator in the personal computer. The time interval between the laser pulses is varied in a range of 9 ~ 16 ms. The observation was made by a monochrome digital CCD camera having a spatial resolution of 1008 × 1018 with 8 bits in gray level, which was synchronized with the pulse signal from the pulse generator and the lasers. The digital image was stored on a frame memory in a personal computer. The sizes of the target images in the present experiment are 120 × 120 mm for imaging the flow over the airfoil and 80 × 80 mm in the airfoil wake, so that the spatial resolution of the captured images are 0.12 mm/pixel and 0.08 mm/pixel, respectively.

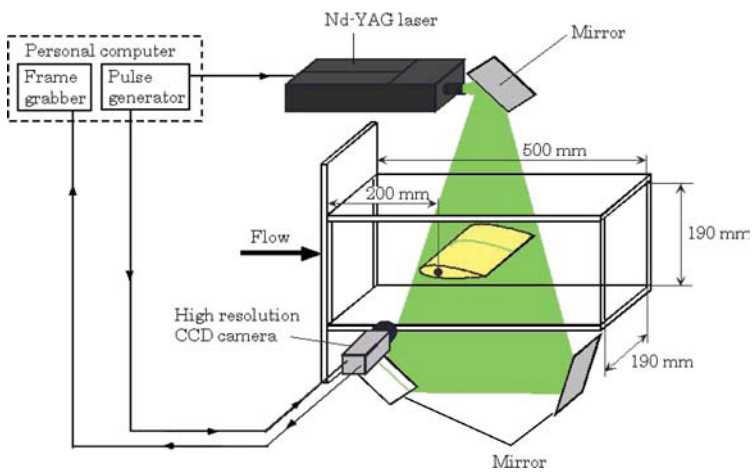

Fig. 2. Experimental test section for flow visualization.

The instantaneous velocity distributions are analyzed by using a gray level difference method for the cross-correlation calculation of the two images. The sizes of interrogation window and search window are set to 60 × 60 pixels and 70 × 70 pixels, respectively, whose combination is found to minimize the error vectors with minimum spatial resolution. The sub-pixel interpolation process is incorporated into this analysis to improve the accuracy of the velocity measurement. The uncertainty in the present velocity measurement is estimated to be about 3% with 95% confidence.

3. Results and Discussion

3.1 Characteristics of Aerodynamic Noise

Figure 3 shows the spectrum of the aerodynamic noise generated from the airfoil at various angles of attack a = 0~15°, which is measured by a sound level meter located at the top wall of the wind tunnel. In most of the attack angles, the sound spectrum does not indicate any peak in the spectrum, but it shows a high peak at a primary frequency of 2.3 ~ 2.4 kHz and a low peak at a double frequency of 4.6 ~ 4.8 kHz when the angle of attack is set to a = 3 ~ 6°. The primary frequency corresponds to Strouhal number St (= $2fd/U$) = 0.16 (d: the thickness of laminar boundary layer at the trailing edge of the airfoil), which agrees closely with the previous experiments by Paterson et al. (1973) indicating the appearance of discrete frequency noise. Therefore, the peak spectrum observed in the present experiment is considered to be due to the generation of the discrete frequency noise. It is to be noted that the noise spectra at larger angles a = 9 ~ 15° become more uniform in distribution, which is reflected by an increase in the separating region of the flow over the suction side of the airfoil. For further details see Fujisawa et al. (2001).

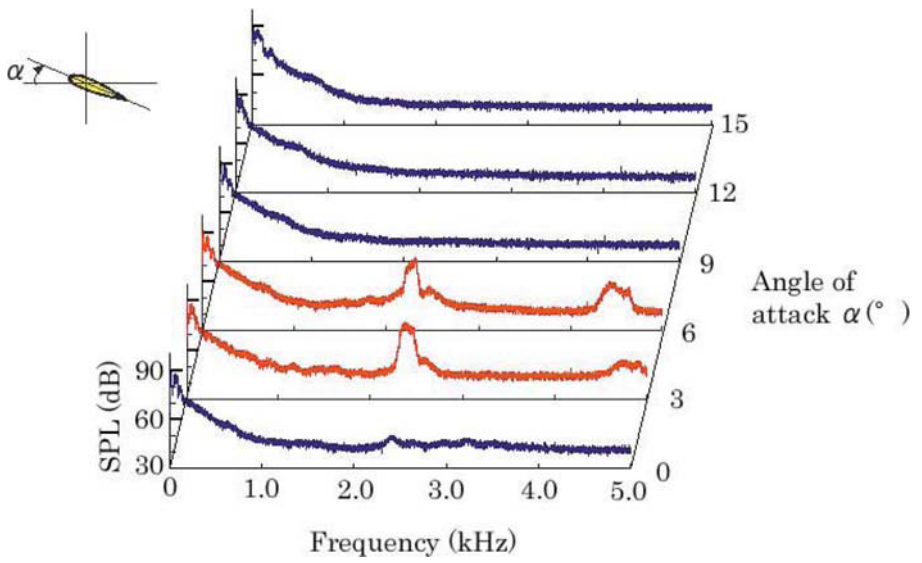

Fig. 3. Noise spectrum of NACA0018 at $Re = 1.6 \times 10^5$.

3.2 Mean Velocity Distributions around Airfoil

The mean velocity distribution around an airfoil was measured by using PIV in the present experiment. A typical result is shown in Fig. 4 for the flow field at three different angles of attack $a = 0^\circ$, 6° and 12°. The present result is obtained by time-averaging 300 sets of instantaneous velocity maps. The points of flow separation, reattachment and reseparation depicted in this figure are obtained from the surface-flow visualization by Fujisawa et al. (2001). It is to be noted that x and y are streamwise and normal distances measured from the axis of the airfoil, respectively, U and V are corresponding mean velocities, respectively and L is a chord length of the airfoil. The velocity distribution at $a = 0^\circ$ roughly shows a symmetrical distribution of the axis of the airfoil. The low velocity region prevails in the upstream of the airfoil, which indicates the presence of the stagnation region of the airfoil.

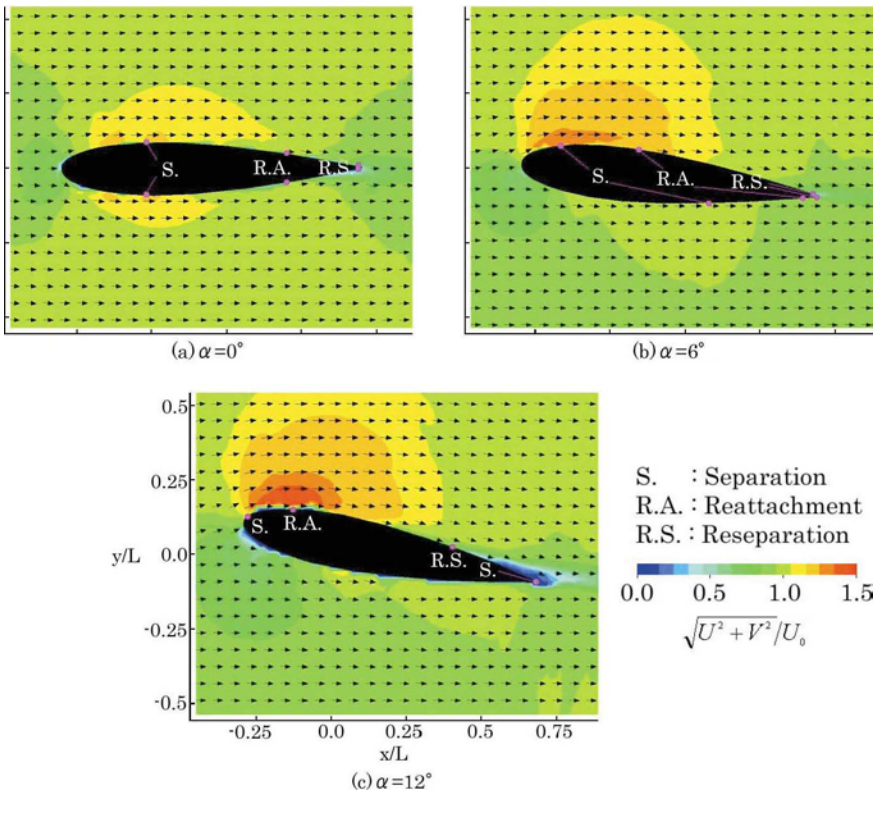

Fig. 4. Mean velocity distributions and contour of velocity magnitude around airfoil.

On the other hand, the velocity over the airfoil section is increased in a short distance from the leading edge due to the displacement effect of the airfoil and it decreases along the airfoil toward the trailing edge. The flow velocity in the downstream of the airfoil becomes lower than the surroundings, which indicates the presence of the airfoil wake. These are general features of the flow around an airfoil and agree closely with those of the previous measurements (Fujisawa and Shibuya, 2001). However, it is rather difficult to observe the points of separation and reattachment from the measured velocity distributions, which is due to the coarse spatial resolution in the present PIV analysis to resolve the fine structure of the boundary layers close to the airfoil surface.

When the angle of attack increases to $a = 6^{\circ}$, the stagnation region moves slightly to the pressure side of the airfoil. At the same time, the magnitude of velocity over the suction side of the airfoil is strengthened, while the local acceleration in the velocity distribution over the pressure side is weakened. It should be mentioned that the region of highest velocity moves upstream in comparison to that at $a = 0^{\circ}$, which coincides with the variation of the separation point observed in the surface flow visualization. On the other hand, the points of separation and reattachment over the pressure side of the airfoil move downstream, which reflects the change of pressure distributions over the pressure side of the airfoil. Such asymmetry of the boundary layers over the suction and pressure side of the airfoil causes the change in the point of reseparation of the boundary layers near the trailing edge. However, the velocity distribution downstream of the airfoil seems to be not so much deviated from that of $a = 0^{\circ}$.

With an increase in the angle of attack to $a = 12^{\circ}$, the flow phenomenon observed at $a = 6^{\circ}$ is more strengthened. Therefore, the stagnation region is enlarged over the leading edge of the pressure side and the velocity over the suction side is accelerated near the leading edge, which results in the corresponding change in the points of flow separation, reattachment and reseparation over the airfoil surface. It is to be noted that the reattachment and reseparation does not appear over the pressure side of the airfoil at $a = 12^{\circ}$, which is due to the short distance of the airfoil surface downstream of the separation point. On the contrary, the flow separation occurs near the trailing edge over the suction side of the airfoil, which agrees closely with the point of reseparation observed by surface flow visualization.

3.3 Instantaneous Flow Structure over Airfoil

In order to understand the instantaneous flow structure over the airfoil, the flow visualization was carried out using a smoke. Illumination was provided by a laser light sheet from Nd:YAG laser. Figure 5 shows the visualized images of the flow over the airfoil at some angles of attack $a = 0^{\circ}$, 6° and 12°. It is to be noted that these visualized images are composed of the two visualizations at different instant, one is taken from the suction side and the other from pressure side. The visualization result at $a = 0^{\circ}$ shows that the dark area is developed from the widest section

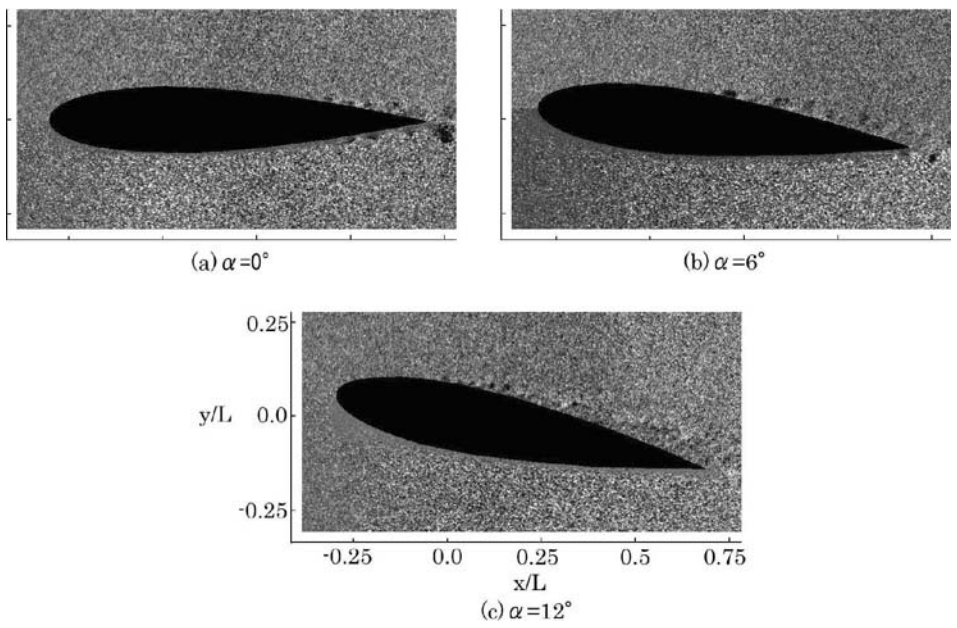

Fig. 5. Visualization of flow structure over airfoil.

of the airfoil and it is attached to the airfoil surface in the downstream. This attachment phenomenon of the boundary layer appears periodically in the rear side of the airfoil. It is to be mentioned that the presence of the dark area in a uniformly distributed smoke can be caused by the presence of large velocity gradients in the local flow with three-dimensional motion (Kompenhans et al., 2000).

With an increase in the angle of attack to $a = 6^{\circ}$, the attached boundary layer prevails over the airfoil, which is shown by the dark cloud pattern over the suction side of the airfoil in a wider range than that at $a = 0^{\circ}$. On the contrary, the flow over the pressure side indicates the generation of dark line from the point of separation and it develops almost straightly to the downstream up to the trailing edge of the airfoil. This dark line seems to be attached to the trailing edge of the airfoil to create counter-clockwise rotating vortices. The generation of such vortices is expected to be related to the discrete frequency noise, since the periodicity of the vortices matches the frequency of the generated noise.

When the angle of attack increases to $a = 12^{\circ}$, the attached boundary layer prevails over most of the suction side of the airfoil and a number of dark clouds formed over the suction side increases, which may suggest the presence of turbulent boundary layer over the rear suction side. On the contrary, the boundary layer over the pressure side of the airfoil remains attached due to the presence of positive pressure gradients. Therefore, the dark separated line was not observed over the pressure side of the airfoil at this angle of attack.

3.4 Instantaneous Flow Structure in Airfoil Wake

The instantaneous flow structure in the wake of the airfoil was studied by flow visualization and PIV analysis. Figure 6 shows the flow visualizations and the corresponding velocity fields downstream of the airfoil at three different angles of attack. The vorticity distributions are also mapped on the velocity distributions, where the

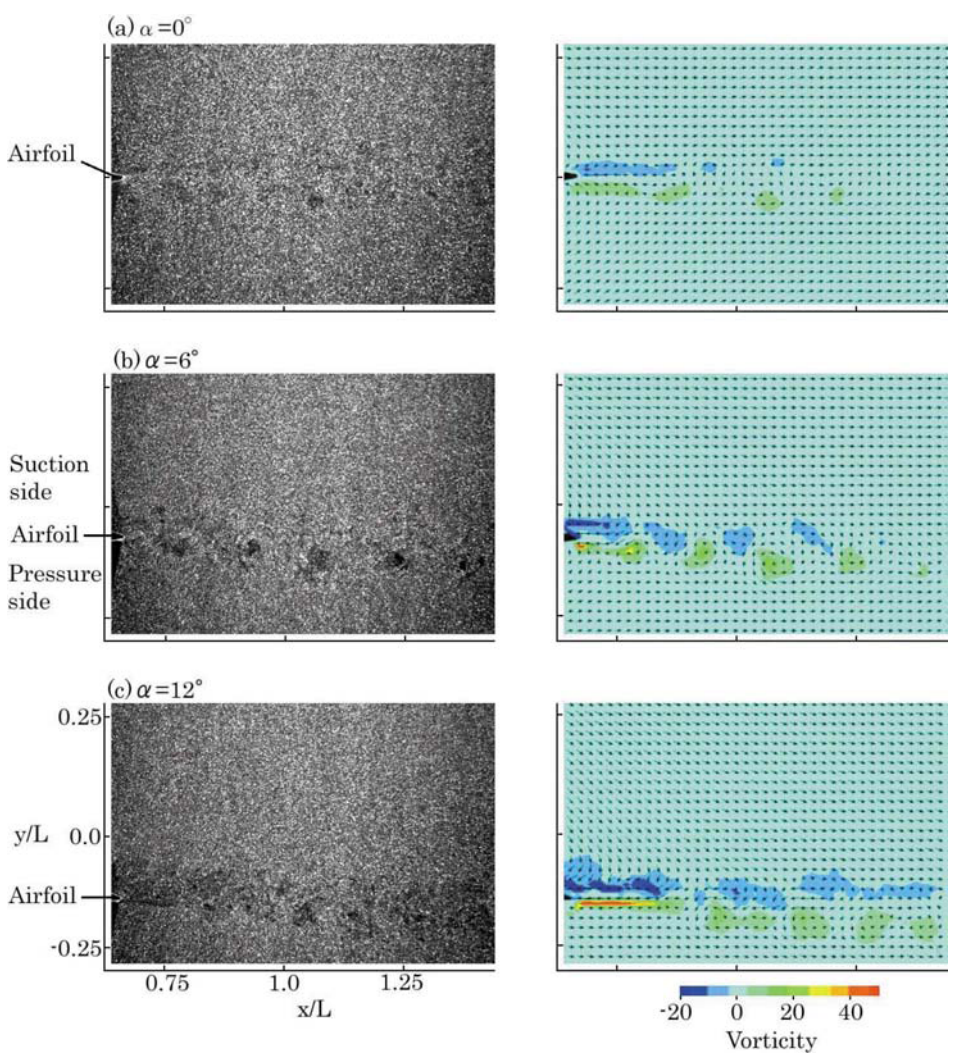

Fig. 6. Instantaneous flow structure in airfoil wake.

vorticity z is defined by $z = L/U_0 (\partial V/\partial x - \partial U/\partial y)$. It should be noted that the velocity distributions are shown by the relative velocity observed from the frame of reference moving at the convection velocity of the vortex street. The convection velocity was found to be 80% of the free-stream velocity, which was obtained from the observation of vortices at $a = 6^\circ$. At the angle of attack $a = 0^\circ$, the smoke visualization does not show any noticeable intensity change in the wake of the airfoil, which suggests small magnitude of vorticity in the wake of the airfoil as seen in the vorticity distributions. This result supports the non-existence of the discrete frequency noise, as seen in Fig. 3.

When the angle of attack increases to $a = 6^\circ$, the smoke shows a periodic pattern, which indicates the evidence of vortex street in the downstream of the airfoil. The formation of the vortex street is more clearly seen in the velocity and vorticity map. It is observed that the counter-clockwise rotating vortex is generated from the pressure side of the airfoil and the position of the vorticity is almost equidistant along the street, which indicates the cyclic nature of the vortex shedding from the airfoil. On the other hand, the clockwise rotating vortex is generated from the suction side of the airfoil, but the magnitude is smaller than that observed from the pressure side. Hence, the vortex street in the wake of the airfoil is asymmetrical in the magnitude of vorticity. It is to be noted that the spacing between the vortices matches with the frequency of the discrete frequency noise observed at this angle of attack.

With an increase in angle of attack to $a = 12^\circ$, the vorticity in the near wake becomes larger but the position of the vorticity becomes irregular, as seen in the velocity and vorticity map. The irregularity of the vortex shedding may be due to the presence of turbulent boundary layer over the suction side of the airfoil and its separation near the rear side of the airfoil. Hence, the occurrence of discrete frequency noise cannot be expected at this angle of attack.

These results indicate that the observation of the flow around the airfoil matches very well with the measurement of aerodynamic noise. The appearance of the discrete frequency noise found at $a = 6^\circ$ can be caused by the interaction of the boundary-layer structure over the suction and pressure side through the trailing edge of the airfoil. However, further study will be needed to explore the details of mechanism on the noise generation by using stereoscopic observation and higher resolution PIV.

4. Conclusion

The characteristics of aerodynamic noise and the physics of the noise generation from a symmetrical airfoil are studied by flow visualization and PIV analysis. The discrete frequency noise was generated from the airfoil when it was inclined to a small angle of attack to the free stream. The flow visualization study of the flow over the airfoil indicated that the aerodynamic noise was generated when the attached boundary layer was formed over the rear suction side and the separated shear layer was produced over the rear pressure side of the airfoil. It was found from the PIV measurements in the airfoil wake that the magnitude of the vorticity developed from the pressure side was larger than that from the suction side, which causes the formation of asymmetrical vortex street in the wake of the airfoil. The periodicity of the shedding vortices in the airfoil wake was found to agree with the frequency of the generated noise.

Acknowledgments

The authors appreciate the experimental help by Messrs. Nakano, T. and Takagi, Y. from Niigata University.

References

Fujisawa, N. and Shibuya, S., Observations of Dynamic Stall on Darrieus Wind Turbine Blades, J. Wind Eng. Ind. Aero., 89-2 (2001), 201-214.

Fujisawa, N., Shibuya, S., Nashimoto, A. and Takano, T., Aerodynamic Noise and Flow Visualization around Two-dimensional Airfoil, to be published in J. Visualization Soc. Jpn., 21-9 (2001), 123-129 (in Japanese).

Hayashi, H., Kodama, Y., Fukano, T. and Ikeda, M., Relationship between Wake Vortex Formation and Discrete Frequency Noise in NACA Blades, Trans. Jpn. Soc. Mech. Engng., 61-B (1995), 2109-2114 (in Japanese).

Hayashi, H., Kodama, Y. and Sasaki, S., Relationship between Discrete Frequency Noises and Wake Vortices on Symmetrical Airfoils, J. Visualization Soc. Jpn., 19-72 (1999), 42-47 (in Japanese).

Kompenhans, J., Raffel, M., Dieterle, L., Dewhirst, T., Vollmers, H., Ehrenfried, K., Willert, C., Pengel, K., Kahler, C., Schroder, A. and Ronneberger, O., Particle Image Velocimetry in Aerodynamics: Technology and Applications in Wind Tunnels, J. Visualization, 2-3/4 (2000), 229-244.

Nakashima, S. and Akishita, S., Discrete Tone Noise on Two-dimensional Wing (Reconstruction of Time Sequential Flow Fluctuation Pattern), Trans. Jpn. Soc. Mech. Engng., 61-B (1995), 2115-2120 (in Japanese).

Paterson, R. W., Vogt, P. G., Fink, M. R. and Munch, C. L., Vortex Noise of Isolated Airfoils, J. Aircraft, 10 (1973), 296-302.

Tam, C. K. W., Discrete Tones of Isolated Airfoils, J. Acoust. Soc. Am., 55-6 (1974), 1173-1177.

Author Profile

Shigeyuki Tomimatsu: He was educated at Kinki University (B.E. 1998) and Graduate School of Kansai University (M.E. 2000). He is now studying at Graduate School of Niigata University as a Ph.D. candidate and continuing the research on PIV for application to aero-acoustics and combusting flow.

Nobuyuki Fujisawa: After he was educated at Tohoku University (M.E. 1979, D.E. 1983), he joined Gunma University in 1983 and worked as a research associate in the field of turbomachinery and turbulence measurement. He was promoted to an associate professor in 1991 and his research field was extended to flow visualization, measurement and control of turbulent flow. Since 1997, he has been a professor of Niigata University and continuing the research on simultaneous measurement of scalar and vector field of thermal and combusting flow, quantitative flow visualization and passive and active control of flow and noise.